Nitrogen and phosphorus release characteristics of pipeline sediments on entering different water bodies

Jiarong Sun [1], Chonghua Xue [1,*], Junqi Li [1,2] and Wenhai Wang[1]

[1] Key Laboratory of Urban Stormwater System and Water Environment, Ministry of Education, Beijing University of Civil Engineering and Architecture, Beijing 100044, China

[2] Beijing Energy Conservation & Sustainable Urban and Rural Development Provincial and Ministry Co-Construction Collaboration Innovation Center, Beijing 100044, China

* Correspondence: xuechonghua@bucea.edu.cn

Abstract: Differences in the physical and chemical properties of reclaimed water (RW) and natural surface water (SW) lead to the differences in terms of nitrogen and phosphorus release when pipeline sediments enter these water bodies. The nitrogen and phosphorus release kinetics from pipe sediments with different particle sizes have been investigated. The results demonstrated that both SW and RW had a pH buffering effect after sediment addition, and the final pH (approximately 8.1) of RW was lower. The release of total phosphorus (TP) and ammonia nitrogen (NH_4^+-N) fitted the first-order kinetic model where the release of TP reached equilibrium; TP release was inhibited in both SW and RW, where RW exhibited the lowest (by a factor of 1.23~2.44) release (0.002 mg/g). The release of NH_4^+-N was promoted in both SW and RW; the maximum release in RW was 0.0188 mg/g. The amounts of NH_4^+-N released in SW and RW were 1.02-1.40 and 1.30-1.80 times that of the control group (CG), respectively. The percentage of TP and NH_4^+-N release in the three groups was highest in 75-154 μm pipe sediment, reaching 34.53% and 43.51% in SW and RW, respectively. These results can assist in the development of water quality evolution models for specific urban scenarios, and provide important guidance for the precise regulation of recharge water quality during and after rainfall.

Key words: pipeline sediment; reclaimed water; surface water; release of TP and NH_4^+-N

1. Introduction

In recent years, water eutrophication has become a rapidly intensifying global environmental crisis [1]. Organic pollutants including nitrogen and phosphorus can enter urban water bodies through stormwater pipe runoff and combined sewer overflow, and are a major cause of water eutrophication [2,3]. Pipeline sediment serves as the principal carrier in the migration and transformation of nitrogen and phosphorus pollutants. The accumulation of nitrogen and phosphorus pollutants in pipes is intensified by rainwater runoff deposits containing particulate matter, and the sediments in rainwater pipes are a sink for nitrogen and phosphorus pollution [4]. During heavy rainfall, the sediments in storm water pipes are discharged into the downstream water body where erosion combined with pipeline runoff releases significant quantities of nitrogen and phosphorus [5,6]. A previous study has established that the contribution of pipeline sediment to nitrogen and phosphorus pollution load in runoff is approximately 30~40% during rainfall events [7]. Moreover, the contribution of pipeline sediments to the organic pollution load is as high as 80% in rainstorm overflow events [8]. Therefore, it is crucial to explore the release of nitrogen and phosphorus when pipeline sediments enter the water body.

With the acceleration of urbanization and the requirement for the implementation of sustainable strategies, urban water environment governance has assumed increasing importance. Due to the lack of available surface water resources in some cities, urban river channels often dry up. In order to maintain

 doi:10.20944/preprints202304.0732.v1

the landscape of urban rivers and lakes and restore the ecology balance, many cities are now actively considering alternative water resources, and reclaimed water is a significant low-cost source of ecological water that can replenish urban rivers and lakes [9]. In Beijing, reclaimed water has become the second most stable water source, and the proportion of reclaimed water that replenishes rivers and lakes has increased from 51.92% in 2012 to 90.97% in 2019 [10]. Although reclaimed water can meet relevant water quality standards after a series of treatments, the use of reclaimed water can also cause some problems. The difference between reclaimed water and surface water lies in its complex composition and higher pollutant concentration. Due to the limitations of reclaimed water treatment technology, the total nitrogen concentration in reclaimed water is higher, and the total phosphorus in reclaimed water is not easy to settle when compared with natural water [11,12]. Environmental factors such as the pH and dissolved oxygen in reclaimed water recharge are also significantly different from those in natural water [13]. Relevant studies have shown that these differences impact on the adsorption, accumulation and release of nitrogen and phosphorus by particulate matter in rainfall runoff [14]. Therefore, in urban watercourses with reclaimed water from sewage plants as the main recharge source, the migration and transformation patterns of rainfall runoff pollutants differ from those in natural watercourses. Application of previous research results and water quality models to urban watercourses with a specific recharge source can result in inaccurate predicted trends with respect to the water environment during and after rainfall. Therefore, it is of immediate practical value to study the transformation mechanism of rainfall runoff pollutants in urban river channels, establishing water quality evolution models that conform to specific urban circumstances, and which allow effective regulation of river water quality during and after rainfall to maintain high urban water environment quality.

Studies on the release of nitrogen and phosphorus from sediments have focused on road sediments, and natural river or lake sediment-water interfaces. Shang et al. investigated the release from road sediments, and found that the particle size distribution of the sediment had a significant effect on the nitrogen and phosphorus release characteristics [15]. Bubba et al. examined the relationship between phosphorus adsorbed in river sediments and sediment particle size, and correlated particle size with phosphorus adsorption [16]. Antelo and Garcia reported that at low pH, particulate matter exhibited a strong adsorption capacity for phosphorus with a gradual decrease in uptake at higher pH, whereas the adsorption capacity of particulate matter for ammonia nitrogen (NH_4^+-N) and organic nitrogen increased with increasing pH [17,18]. Pan et al. have demonstrated that nitrogen and phosphorus release in sediments from a surface water river supply was higher than that from a reclaimed water supply [14]. However, given the relatively short period of time that reclaimed water has been used there are few comparative studies that address possible changes in nitrogen and phosphorus content and water quality due to sediments after they enter surface water and reclaimed water.

In this study, we have undertaken a comparative analysis of nitrogen and phosphorus release by particles of different sizes in three kinds of water (deionized water, reclaimed water (RW) and surface (river) water (SW). The mass fraction and water characteristics have been evaluated. The TP and NH_4^+-N were measured with respect to reaction time, and a first order kinetics model has been applied to quantify the release mechanism.

Preprints (www.preprints.org) | NOT PEER-REVIEWED | Posted: 23 April 2023 doi:10.20944/preprints202304.0732.v1

2. Materials and Methods

2.1. Raw water and pipe sediments

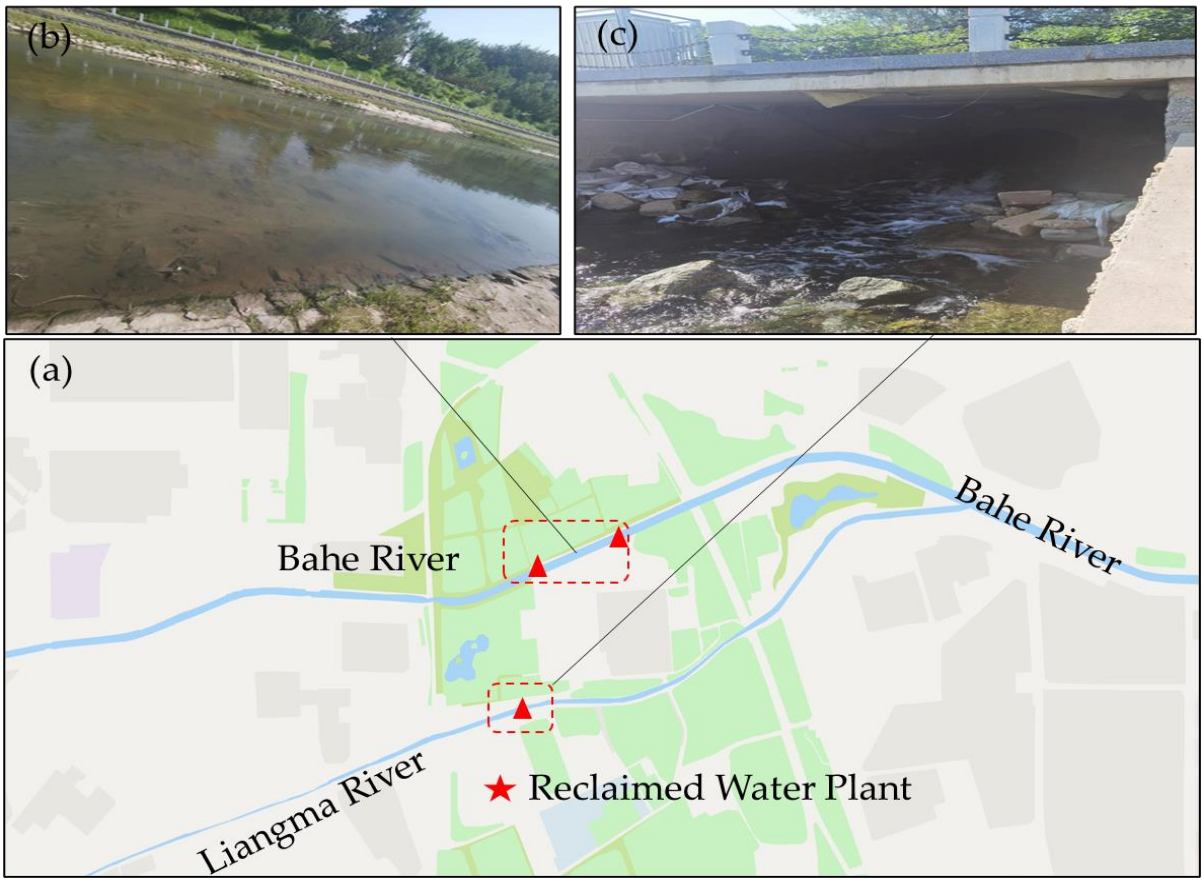

Figure 1. (a) The location of the sampling sites: **(b)** photograph of the river water sampling sites; **(c)** photograph of the reclaimed water sampling sites.

The river water samples were collected from the upper reaches of Bahe River, as illustrated in Figure 1. Bahe River is an important branch of the North Canal system, located in the Dongcheng and Chaoyang districts. It rises in the northeast and eventually merges with the Warm Elm River at Calendula Street. The main tributaries include Beihe River, Liangma River and Beituchenggou. The main river length is 21.63 kilometers, and the drainage area is 158.4 square kilometers. The main sources of replenishment are reclaimed water and natural surface runoff. The river is the main water transport and landscape corridor in Chaoyang District, and also serves as an important flood channel in the central city.

The reclaimed water was collected from Beijing Jiuxianqiao Reclaimed Water Plant (treatment capacity: 200,000 cubic meters/day), located in Jiangtaiwa Village, Dongfeng Township, Chaoyang District, Beijing, as shown in Figure 1(c). The sewage is treated by an oxidation ditch activated sludge, and the reclaimed water is treated by a two-stage biological filter + sand filter/cloth filter. Part of the reclaimed water is used as supplementary water in the Bahe River Basin, and part is delivered to the reclaimed water users through a pipe network. The water samples were all transferred into 2L polyethylene sampling bottles, refrigerated and stored away from light, before being sent to the

Preprints (www.preprints.org) | NOT PEER-REVIEWED | Posted: 23 April 2023 doi:10.20944/preprints202304.0732.v1

laboratory for testing.

The sediments of the pipeline were collected from a rainwater pipeline in a campus in Beijing, August, 2022. The whole pipeline forms a separate stormwater system without a domestic sewage mixed connection. A sampling shovel was used to extract pipeline sediment in the two rainwater Wells of the selected rainwater pipeline. Following collection, the mixed samples were sent to the laboratory for freeze-drying. The dried sediments were passed through a 16-mesh screen to remove impurities. In order to study the nitrogen and phosphorus release characteristics of pipe sediment in different particle size ranges, the dried sediments were screened using 42 mesh, 100 mesh and 200 mesh standard screens successively. The sediment samples were divided into four different particle sizes: > 355 μm, 154-355 μm, 75-154 μm, and < 75 μm. After screening, the sediments were stored at -20 ℃ before use.

2.2. Experimental design

This study sets out to investigate the release characteristics of TP and NH_4^+-N from pipe sediment with different particle sizes in various types of water. The desorption experiment was conducted in a 3 L beaker with 40 g ＞355 μm sediment dispersed under magnetic stirring in three water types (2 L): deionized water as the control group (CG), RW and SW. Samples (50 ml) were collected at intervals of 1, 3, 5, 7, 10, 20, 40, 60, 90, 120, 180, 240, and 300 min. The samples were centrifuged and filtered through a 0.45 μm filtration membrane, then stored in 50 ml polyethylene bottles at 4℃ for a maximum of 24 hours. The remaining sediments, in the size ranges 154-355 μm, 75-154 μm, and < 75 μm, were sampled following the same protocol.

2.3. Analytical Techniques

The pH was measured using a portable multi-parameter water quality analyzer (American Hach HQ-40d, Hach Company (Loveland, CO, USA)). The concentrations of TP and NH_4^+-N in water were determined by applying the ammonium molybdate spectrophotometric method and the salicylic acid spectrophotometric method, respectively

Due to the complexity of nitrogen and phosphorus components in particulate matter, some of the nitrogen and phosphorus will not be released after entering water, notably calcium-bound phosphorus and some organic nitrogen which is difficult to degrade. Therefore, we determined the alkali-hydrolyzable nitrogen, available phosphorus and ammonia nitrogen in sediments [19]. Alkali-hydrolyzable nitrogen includes inorganic nitrogen (ammonium nitrogen, nitrate nitrogen) and organic nitrogen that is readily hydrolyzed. Available phosphorus includes all water-soluble phosphorus, some adsorbed phosphorus, some slightly soluble inorganic phosphorus and mineralized organic phosphorus. The alkali-hydrolyzable nitrogen content and ammonia nitrogen content in sediments were measured by potassium chloride solution extraction and spectrophotometry. The quantity of available phosphorus in sediments was determined by sodium bicarbonate extraction and the molybdenum-antimony anti-spectrophotometric method.

2.4. Data Analysis

The release of TP and NH_4^+-N in sediments was calculated according to formula (1).

Preprints (www.preprints.org) | NOT PEER-REVIEWED | Posted: 23 April 2023 doi:10.20944/preprints202304.0732.v1

$$Q=\frac{(C_e-C_0)V}{m} \quad (1)$$

where C_0 is the initial concentration of river water and reclaimed water (mg/L), C_e is the concentration after a given time interval (mg/L), V is the solution volume, and m is the weight of the pipe sediment (L).

The kinetic curve for the desorption of nitrogen and phosphorus from particles can be expressed by the first order kinetic equation [20].

$$Q=E*(1-e^{-bt-a}) \quad (2)$$

where E is the desorption amount at equilibrium (mg/g), b is the desorption rate constant which reflects the degree of pollution, t is the desorption time (min) and a is constant.

3. Results and Discussion

3.1. Pollution characteristics of water samples and pipe sediments

The mass fraction of the four kinds of pipe sediment with different particle sizes is shown in Table 1. It should be noted that the highest proportion of particles was in the size range 154~355 μm, accounting for a mass fraction of 36.04%. The sediment content of ＜ 355 μm was the lowest, with a mass fraction of 14.86% and there was a near equivalence of particles ＜75 μm (22.44%) and in the 75-154 μm range (26.66%). Although most of the sediment in stormwater pipes comes from ground surface sediments, the sample particle size distribution differs from ground surface sediment size characteristics. Surface sediments typically show the largest proportion of particles less than 75 μm [21] as opposed to the predominant larger grain size (154~355 μm) found in pipe sediments (Table 1). This may be due to differences in the internal environment of the pipeline. Smaller particles are more likely to be washed away while large particles are retained [22].

Table 1. Mass fraction of pipe sediments with different particle sizes.

Particle size range (μm)	Proportion (%)
＞355	14.86
154-355	36.04
75-154	26.66
＜75	22.44

The content of nitrogen and phosphorus pollution load in sediments of different particle sizes is shown in Figure 2(a). It should be noted that the smaller the sediment particle size, the higher the content of nitrogen and phosphorus nutrients per unit mass. Sediments with particle sizes smaller than 75 μm exhibited the highest pollution load of alkali-hydrolyzable nitrogen, available phosphorus, and ammonia nitrogen with percentages of 0.112 mg/g，0.011 mg/g 和 0.046 mg/g, respectively. These results are in agreement with a previous study [23]. At a smaller particle size, the specific surface area is larger which should provide a greater adsorption capacity for nitrogen and phosphorus [24].

According to the mass fraction of sediments with different particle sizes in Table 1, The pollution load ratio was used to measure the contribution of different particle size sediment to the total pollution of pipeline. Calculate according to formula (3).

$$GSF_{Load}(\%)=\frac{C_i\times GS_i}{\sum_{i=1}^{n} C_i\times GS_i} \quad (3)$$

where C_i is the mass fraction of pollutant in particle size fraction i (mg/g), GS_i is the mass fraction of particle size fraction i (%), n is the number of particle groups and n is taken as 4 in this paper.

Preprints (www.preprints.org) | NOT PEER-REVIEWED | Posted: 23 April 2023 doi:10.20944/preprints202304.0732.v1

The weighted nitrogen and phosphorus pollution loads are shown in Figure 2(b). The maximum alkali-hydrolyzed nitrogen pollution load occurred in 75-154 μm pipeline sediments (32%), and the maximum available phosphorus and ammonia nitrogen pollution load was found in the sediment of < 75 μm (39%) and 154-355 μm (31%). Although the smaller particle size pipe sediment had a higher nitrogen and phosphorus pollution load as shown in Figure 2(a), the difference in the mass fraction of pipe sediment with different particle sizes resulted in a different final weighted nitrogen and phosphorus pollution load. This is in agreement with a previous study [25].

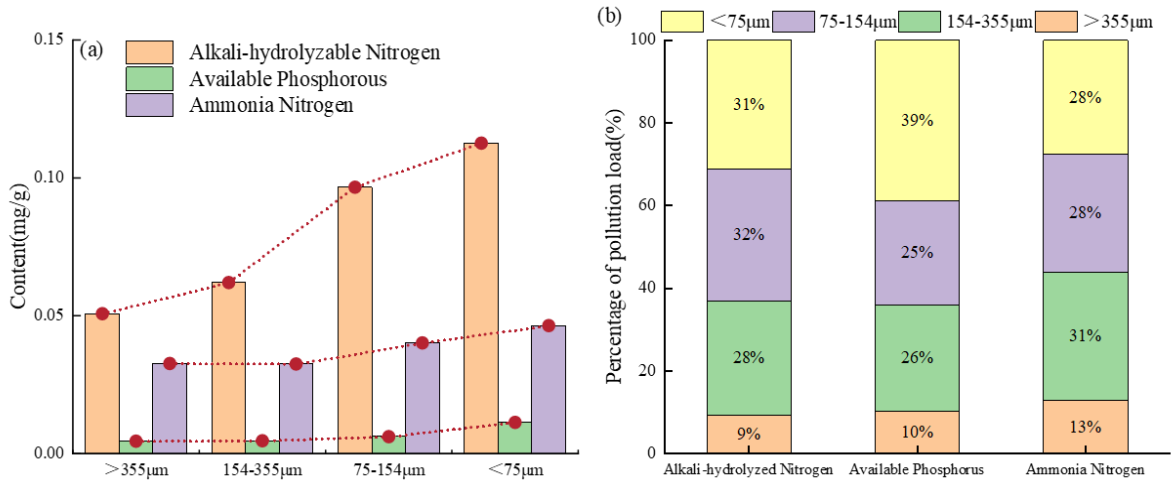

Figure 2. **(a)** Nitrogen and phosphorus mass fraction and **(b)** pollution load percentage in different particle size pipeline sediments.

3.2. Change of pH in water before and after reaction

Figure 3 shows the pH variation in the three types of water bodies before and after the addition of sediment (denoted as BE and AF, respectively). It should be noted that the highest pH was recorded for SW before addition of sediment, and the pH of the RW was higher than the CG. This may be attributed to a depletion of CO_2 due to photosynthesis by phytoplankton in RW [26]. After the addition of sediment, the pH of the three water bodies all increased. The starting pH of the CG was 7.1±0.2 which was raised to 9.3±0.1 following the inclusion of sediment. In the case SW, the pH was increased from 8.9±0.1 to 9.0±0.1, which compares with an increase in the pH of RW from 7.6±0.2 to 8.1±0.1 due to sediment addition. The final pH followed the sequence CG > SW > RW, which is consistent with the research results reported by Hou et al. [10]. Compared with the CG, the pH variation in the case of SW and RW was significantly smaller. According to previous studies, this response can be ascribed to the presence of various ions in river water and reclaimed water formed by different acid-base buffer systems, such as carbonate, sulfate and Al(Ⅲ) buffers [27]， which played a role in buffering possible pH changes in water.

Preprints (www.preprints.org) | NOT PEER-REVIEWED | Posted: 23 April 2023 doi:10.20944/preprints202304.0732.v1

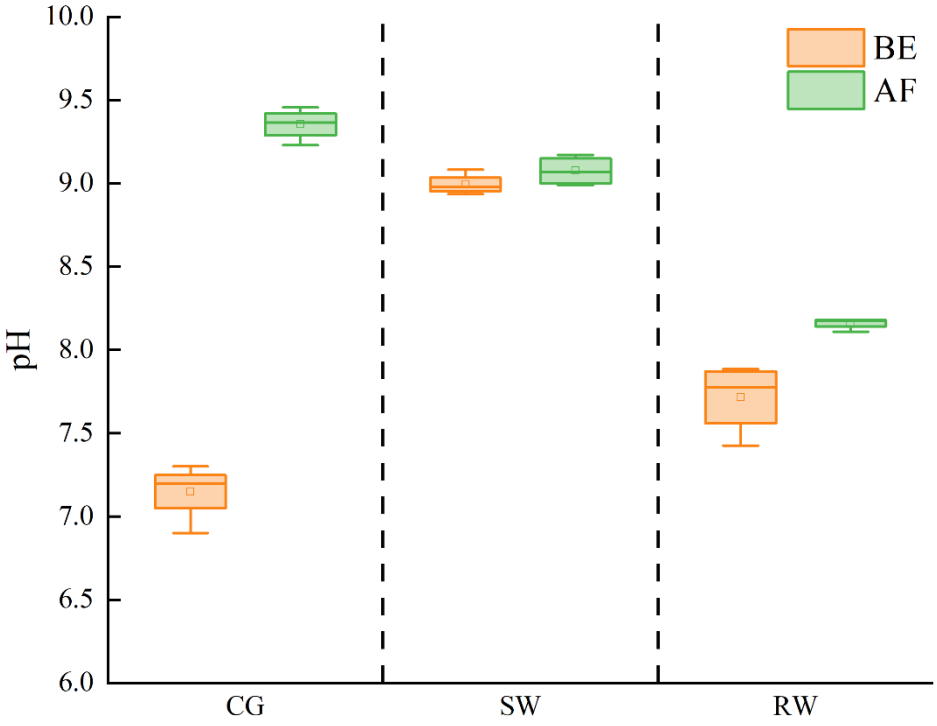

Figure 3. Changes in pH of different water bodies before and after pipeline sediment addition.

3.3. The release characteristics of TP

The relationship between TP release in different water bodies and pipe sediment particle sizes is shown in Figure 4. Initially, due to the large gap in TP concentration between the sediments and the accommodating waters, the TP release showed a marked increase and, at extended reaction times, the release rate decreased to reach a plateau value representing equilibrium after 120 min. As illustrated in Figure 4(a) - (d), it should be noted that at equilibrium, the amount of TP released was higher in every case for the CG when compared with SW and RW. The amount of TP released in the CG was 1.06-1.56 times that of SW and 1.23-2.44 times that of RW. The results indicate that TP release was inhibited in both SW and RW, especially in RW which exhibited the lowest release (0.002 mg/g).

Preprints (www.preprints.org) | NOT PEER-REVIEWED | Posted: 23 April 2023 doi:10.20944/preprints202304.0732.v1

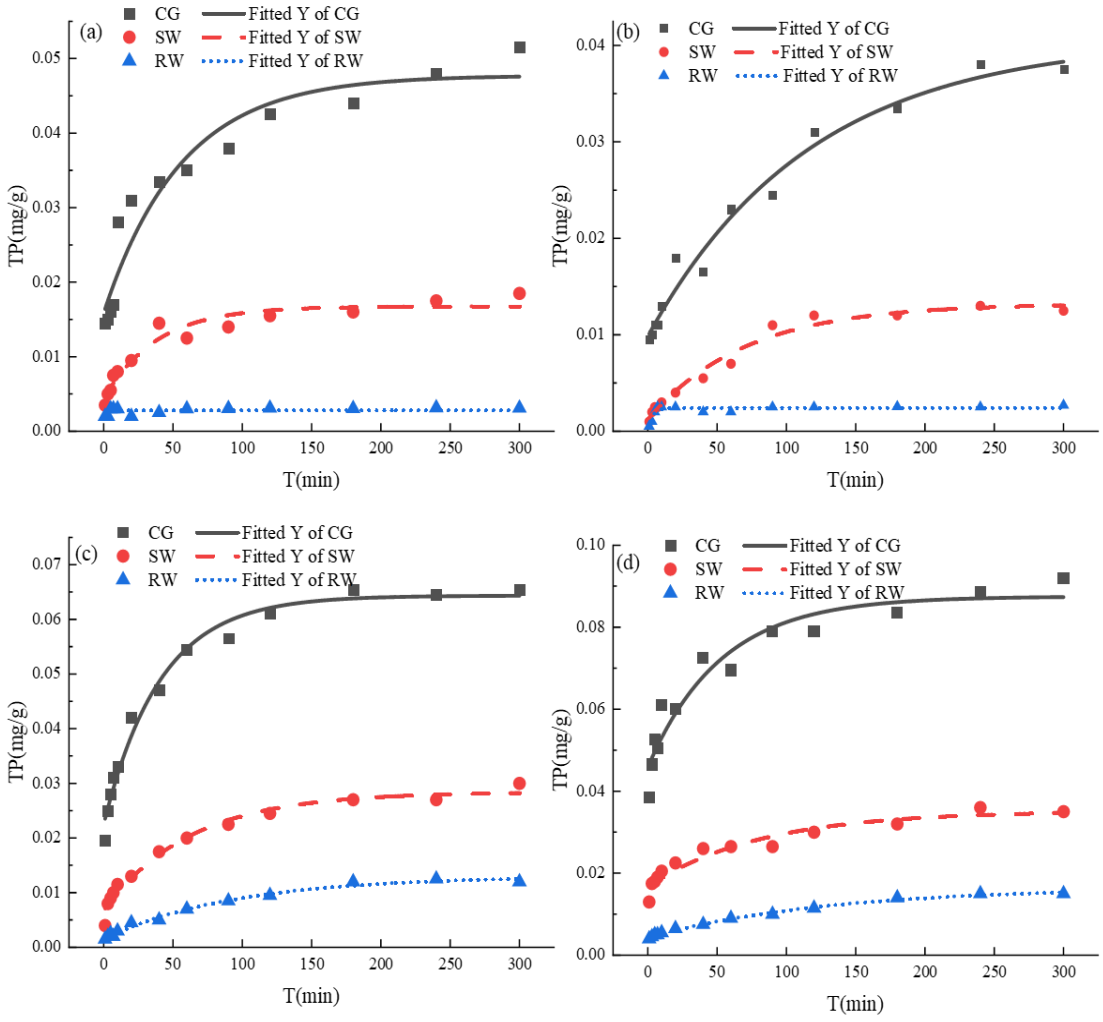

Figure 4. TP release kinetics curves for pipeline sediment with different particle sizes: **(a)** > 355 μm; **(b)** 154-355 μm; **(c)** 75-154 μm; **(d)** < 75 μm.

In order to further investigate the release kinetics of TP in sediments with different particle sizes, the first-order reaction kinetics model was used for data fitting, as shown in Table 2. It should be noted that the ultimate TP release at equilibrium for the different sediment particle size decreased in the order, E (< 75 μm) > E (75-154 μm) > E (> 355 μm) > E (154-355 μm). On the basis of R^2 , TP desorption from different particle sizes in different waters was in accordance with the primary reaction kinetic characteristics. Therefore, it can be inferred that the release of TP was mainly controlled by physical desorption [28].

The suppression of TP release in SW and RW may be due to the higher TP concentration in SW and RW which inhibited ionic diffusion of phosphate in the particulate matter. Moreover, the variation of pH in the different water samples (as displayed in Figure 3) has established that the pH in SW and RW after reaction was lower than that in the CG. At a lower water pH, the surface of the particulate matter exhibits a greater positive charge. The greater electrostatic attraction generated by the positive charge favors phosphate adsorption [29]. In addition, the lower pH impeded the binding of Fe^{3+} and Al^{3+} to OH^-, hindering the release of Fe-P and Al-P from the particulate matter. A previous study has also suggested that organic matter in water can bridge with Fe^{3+} and Al^{3+} and other metal ions, combining

Preprints (www.preprints.org) | NOT PEER-REVIEWED | Posted: 23 April 2023 doi:10.20944/preprints202304.0732.v1

with phosphorus to form stable organic-metal chelates which favors the adsorption of phosphorus on particulate matter [30].

Table 2. First-order reaction kinetic model fitting parameters for the desorption of TP from particulate matter.

	classification	E(mg/g)	b	a	R^2
＞355 μm	CG	0.047	0.027	0.38	0.92
	SW	0.016	0.026	0.25	0.94
	RW	0.003	0.022	0.19	0.93
154-355 μm	CG	0.041	0.018	0.28	0.98
	SW	0.013	0.014	0.07	0.98
	RW	0.002	0.004	0.37	0.85
75-154 μm	CG	0.064	0.024	0.42	0.98
	SW	0.028	0.015	0.25	0.97
	RW	0.013	0.010	0.12	0.98
＜75 μm	CG	0.087	0.018	0.73	0.93
	SW	0.035	0.012	0.64	0.92
	RW	0.016	0.007	0.26	0.99

3.4. The release characteristics of NH_4^+-N

The release kinetics of NH_4^+-N from pipeline sediments with different particle sizes in different water bodies are presented in Figure 5. The release process of NH_4^+-N release can be divided into two stages: fast reaction and slow reaction. The amount of NH_4^+-N released gradually approached an invariable value with increasing reaction time. The NH_4^+-N released (0.0188 mg/g) in RW from pipeline sediments was higher than that in SW and the CG, as shown in Figure 5(d). The release of NH_4^+-N in SW was also higher than that in the CG. This indicates that the release of NH_4^+-N in particulate matter was promoted in SW and RW, and the greater release of NH_4^+-N in RW can be linked to the lowest pH in RW. When the pH was raised to 7.0, it exceeded the charge zero of the submerged mud colloid, rendering the surface of the particulate matter negatively charged. The higher the pH, the more favorable the adsorption of particulate matter NH_4^+ , thus inhibiting release of NH_4^+-N to the surrounding water. At the same time, H^+ at the lower pH competes strongly for NH_4^+ in the mud colloid and contributes to desorption.

Preprints (www.preprints.org) | NOT PEER-REVIEWED | Posted: 23 April 2023 doi:10.20944/preprints202304.0732.v1

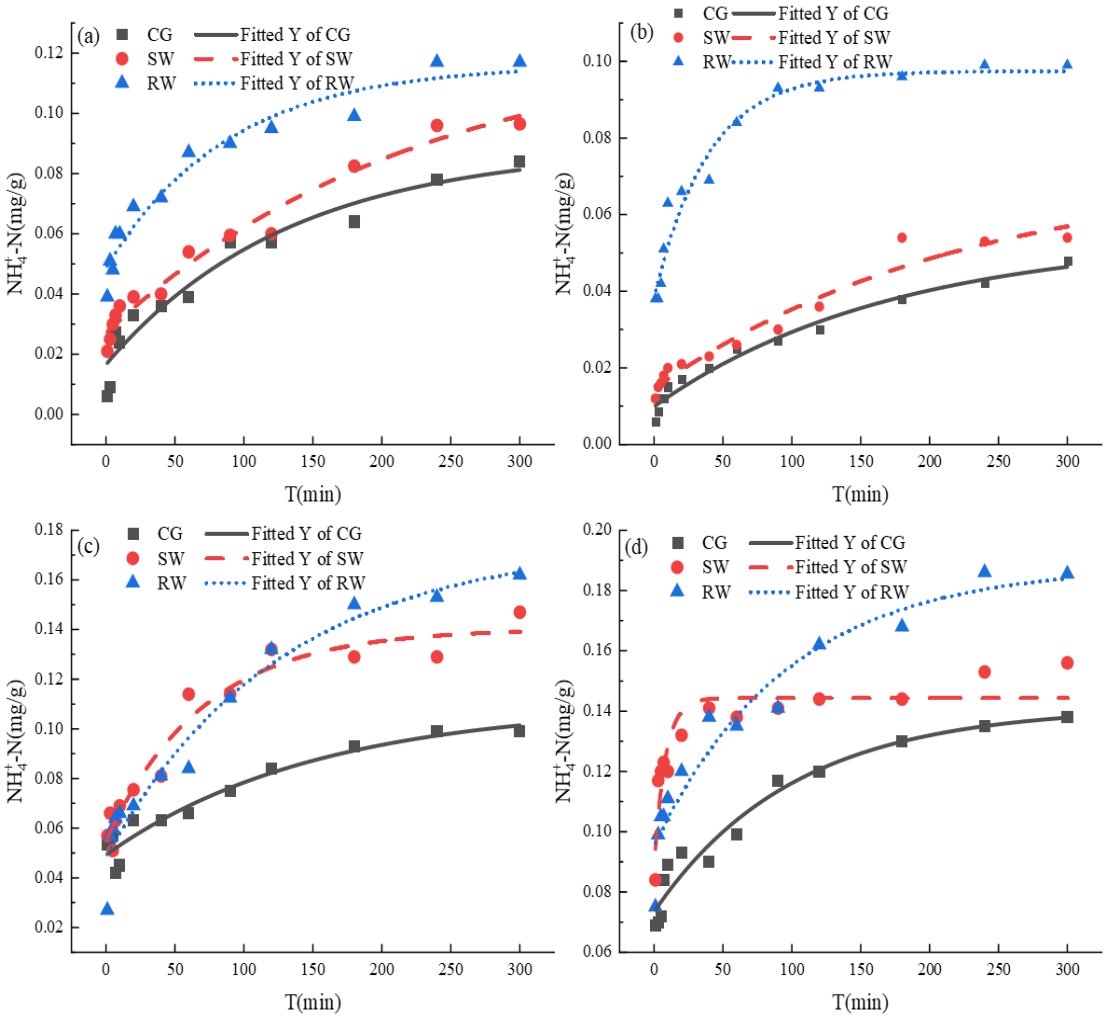

Figure 5. NH_4^+-N release kinetics curves for pipeline sediments with different particle sizes: **(a)** > 355 μm; **(b)** 154-355 μm; **(c)** 75-154 μm; **(d)** < 75 μm.

The first-order reaction kinetics model (equation (2)) was used to fit the NH_4^+-N data; the fitting parameters are given in Table 3. It should be noted that the NH_4^+-N release at reaction equilibrium for different particle sizes of sediment decreased in the order E (< 75 μm) > E (75-154 μm) > E (> 355 μm) > E (154-355 μm). According to R^2 , the release of NH_4^+-N in pipeline sediments conformed to the first-order reaction kinetics model with a high correlation coefficient. Therefore, the release of NH_4^+-N was also mainly controlled by physical desorption [20].

Preprints (www.preprints.org) | NOT PEER-REVIEWED | Posted: 23 April 2023 doi:10.20944/preprints202304.0732.v1

Table 3. The first-order reaction kinetic model fitting parameters for the desorption of NH_4^+-N from particulate matter.

	classification	E (mg/g)	b	a	R^2
>355 μm	CG	0.0088	0.008	0.21	0.94
	SW	0.0115	0.004	0.16	0.97
	RW	0.0116	0.011	0.54	0.95
154-355 μm	CG	0.0054	0.005	0.20	0.98
	SW	0.0071	0.004	0.23	0.96
	RW	0.0097	0.025	0.51	0.96
75-154 μm	CG	0.0109	0.006	0.59	0.94
	SW	0.0140	0.014	0.49	0.95
	RW	0.0174	0.007	0.32	0.96
<75 μm	CG	0.0141	0.009	0.73	0.96
	SW	0.0144	0.125	0.93	0.85
	RW	0.0188	0.012	0.70	0.94

3.5. Percentage of TP and NH_4^+-N released by different particle size pipe sediment

Taking the maximum released amounts of TP and NH_4^+-N recorded in Table 2 and Table 3, and the content of available phosphorus and ammonia nitrogen in the different particle size sediment, the percentage release was calculated, and is presented in Figure 6. It should be noted that the sediment in the size range 75-154 μm exhibited the highest percentage of TP and NH_4^+-N release into the three water samples. The percentage release of both TP and NH_4^+-N was lowest in the 154-355 μm sediment size range. In addition, the percentage of TP release from 75-154 μm sediment was the highest in the CG (34.53%), while the percentage NH_4^+-N release from 75-154 μm particles was the highest in RW (43.51%). Therefore, 75-154 μm pipe sediments exhibited the greatest risk of contamination. The percentage release of TP in CG was 2.01-3.08 times that in SW, and 5.21-15.97 times that in RW.

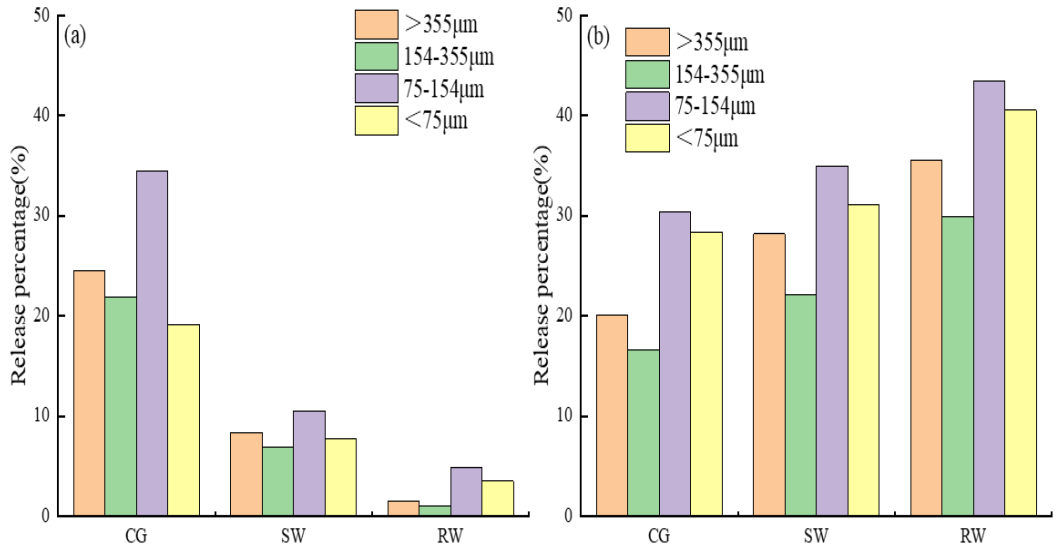

Figure 6. The percentage release of **(a)** TP and **(b)** NH_4^+-N in sediments with different particle sizes.

4. Conclusions

This study has explored nitrogen and phosphorus release characteristics from sediment with different particle sizes after entering different water bodies. The results generated to support the following conclusions. The mass fraction of 154-355 μm particles in the pipeline sediments was the largest. Although the sediment with a smaller particle size can accumulate more pollutants, the pollution load of weighted NH_4^+-N and TP was the highest in the sediment of 75-154 μm size range. Both the release of TP and NH_4^+-N from pipeline sediments conformed to the first-order reaction kinetics model. The release of TP was inhibited in SW and RW to varying degrees, and RW exhibited a stronger inhibition of TP release. NH_4^+-N release was promoted in SW and RW, and RW showed a stronger promotional effect with respect to NH_4^+-N. The TP and NH_4^+-N percentage release was highest for sediment in the size range 75-154 μm. Therefore, attention should be paid to the characteristics of runoff pollution into different water bodies as possible recharging sources in order to control and manage urban water pollution. The long-term pollution characteristics of runoff pollution after entering different water bodies and the associated ecological risks warrant further study.

Author Contributions: Data curation, J.S.; writing—original draft preparation, J.S. and C.X.; writing—review and editing, J.S. and C.X.; supervision, J.L. and W.W. All authors have read and agreed to the published version of the manuscript.

Funding: This research was funded by the National Natural Science Foundation of China, grant number 2021YFC3200701.

Institutional Review Board Statement: Not applicable.

Informed Consent Statement: Not applicable.

Data Availability Statement: Not applicable.

Conflicts of Interest: The authors declare no conflict of interest.

Reference:

1. Spears, B.M.; Carvalho, L.; Perkins, R.; Kirika, A.; Paterson, D.M. Sediment phosphorus cycling in a large shallow lake: spatio-temporal variation in phosphorus pools and release. In Proceedings of the Shallow Lakes in a Changing World: Proceedings of the 5th International Symposium on Shallow Lakes, held at Dalfsen, The Netherlands, 5–9 June 2005, 2007; pp. 37-48.
2. Paerl, H.W.; Scott, J.T.; McCarthy, M.J.; Newell, S.E.; Gardner, W.S.; Havens, K.E.; Hoffman, D.K.; Wilhelm, S.W.; Wurtsbaugh, W.A. It takes two to tango: when and where dual nutrient (N & P) reductions are needed to protect lakes and downstream ecosystems. *Environ Sci Technol* **2016**, *50*, 10805-10813.
3. Lewis Jr, W.M.; Wurtsbaugh, W.A.; Paerl, H.W. Rationale for control of anthropogenic nitrogen and phosphorus to reduce eutrophication of inland waters. *Environ Sci Technol* **2011**, *45*, 10300-10305.
4. Aryal, R.; Jinadasa, H.; Furumai, H.; Nakajima, F. A long‐term suspended solids runoff simulation in a highway drainage system. *Water science & technology* **2005**, *52*, 159-167.
5. Chang, S.; Tang, Y.; Dong, L.; Zhan, Q.; Xu, W. Impacts of sewer deposits on the urban river sediment after rainy season and bioremediation of polluted sediment. *Environ Sci Pollut R* **2018**, *25*, 12588-12599.
6. Xu, Z.; Xiong, L.; Li, H.; Yin, H.; Wu, J.; Xu, J.; Zhang, J. Pollution characterization and source analysis of the wet weather discharges in storm drainages. *Desalin Water Treat* **2017**, *72*, 169-181.
7. Gasperi, J.; Gromaire, M.C.; Kafi, M.; Moilleron, R.; Chebbo, G. Contributions of wastewater, runoff and sewer deposit erosion to wet weather pollutant loads in combined sewer systems. *Water Res* **2010**, *44*,

5875-5886, doi:10.1016/j.watres.2010.07.008.

8. Ahyerre, M.; Chebbo, G. Identification of in-sewer sources of organic solids contributing to combined sewer overflows. *Environmental technology* **2002**, *23*, 1063-1073.
9. Chu, J.; Chen, J.; Wang, C.; Fu, P. Wastewater reuse potential analysis: implications for China's water resources management. *Water Res* **2004**, *38*, 2746-2756.
10. Ying, H.; Xin, L.; Ling, B.; Yi-juan, B.; Shu-rong, Z.; Sheng-rui, W.; Lei, Z.; Ai-zhong, D. Phytoplankton Community Structures and Its Relationship with Environmental Factors in Rivers Supplied with Different Water Sources. *Environmental Science* **2022**, *43*, 5616-5626, doi:10.13227/j.hjkx.202202218.(In Chinese)
11. Lv, X.; Zhang, J.; Liang, P.; Zhang, X.; Yang, K.; Huang, X. Phytoplankton in an urban river replenished by reclaimed water: Features, influential factors and simulation. *Ecol Indic* **2020**, *112*, 106090.
12. Liu, W.; Xu, Z.; Long, Y.; Feng, M. Replenishment of urban landscape ponds with reclaimed water: Spatiotemporal variations of water quality and mechanism of algal inhibition with alum sludge. *Sci Total Environ* **2021**, *790*, 148052.
13. Yang, L.; He, J.; Liu, Y.; Wang, J.; Jiang, L.; Wang, G. Characteristics of change in water quality along reclaimed water intake area of the Chaobai River in Beijing, China. *Journal of environmental sciences* **2016**, *50*, 93-102.
14. Fan, P.; Wang, Y.; Wang, W.H.; Chai, B.H.; Lu, X.X.; Zhao, J.C. Release characteristics of nitrogen and phosphorus from sediments formed under different supplemental water sources in Xi'an moat, China. *Environ Sci Pollut R* **2019**, *26*, 10746-10755, doi:10.1007/s11356-019-04537-z.
15. Limin, S.; Jianlong, W.; Yajun, Z. Characteristics of nitrogen and phosphorus dissolved from urban road-deposited sediment. *Chinese Journal of Environmental Engineering* **2014**, *8*, 891-896.(In Chinese)
16. Del Bubba, M.; Arias, C.; Brix, H. Phosphorus adsorption maximum of sands for use as media in subsurface flow constructed reed beds as measured by the Langmuir isotherm. *Water Res* **2003**, *37*, 3390-3400.
17. Antelo, J.; Avena, M.; Fiol, S.; López, R.; Arce, F. Effects of pH and ionic strength on the adsorption of phosphate and arsenate at the goethite-water interface. *J Colloid Interface* **2005**, *285*, 476-486.
18. Garcia, C.; Hernandez, T.; Costa, F.; Ceccanti, B.; Ciardi, C. Changes in ATP content, enzyme activity and inorganic nitrogen species during composting of organic wastes. *Canadian Journal of Soil Science* **1992**, *72*, 243-253.
19. Toor, G.S.; Occhipinti, M.L.; Yang, Y.Y.; Majcherek, T.; Haver, D.; Oki, L. Managing urban runoff in residential neighborhoods: Nitrogen and phosphorus in lawn irrigation driven runoff. *Plos One* **2017**, *12*, e0179151, doi:10.1371/journal.pone.0179151.
20. Balci, S. Nature of ammonium ion adsorption by sepiolite: analysis of equilibrium data with several isotherms. *Water Res* **2004**, *38*, 1129-1138, doi:10.1016/j.watres.2003.12.005.
21. German, J.; Svensson, G. Metal content and particle size distribution of street sediments and street sweeping waste. *Water Sci Technol* **2002**, *46*, 191-198.
22. Hu, L.; Zhao, H. Influence of particle size on diffuse particulate pollutants in combined sewer systems. *Science of the Total Environment* **2022**, *846*, 157476, doi:10.1016/j.scitotenv.2022.157476.
23. Vaze, J.; Chiew, F.H. Nutrient loads associated with different sediment sizes in urban stormwater and surface pollutants. *Journal of Environmental Engineering* **2004**, *130*, 391-396.
24. Hou, P.; Ren, Y.; Zhang, Q.; Lu, F.; Ouyang, Z.; Wang, X. Nitrogen and Phosphorous in Atmospheric Deposition and Roof Runoff. *Polish Journal of Environmental Studies* **2012**, *21*.
25. Aiyi, Z.; Jian, Y. Pollutants exchange characteristics of sediment-water interface in Zhuzhou rainwater pipeline. *Chinese Journal of Environmental Engineering* **2021**, *15*, 2322-2332.(In Chinese)
26. Yang, L.; He, J.; Liu, Y.; Wang, J.; Jiang, L.; Wang, G. Characteristics of change in water quality along

 doi:10.20944/preprints202304.0732.v1

reclaimed water intake area of the Chaobai River in Beijing, China. *J Environ Sci (China)* **2016**, *50*, 93-102, doi:10.1016/j.jes.2016.05.023.

27. Stumm, W.; Morgan, J.J.; Drever, J.I. Aquatic chemistry. *J Environ Qual* **1996**, *25*, 1162.
28. Sulin, X.; Taozhe, W.; Congyuan, G.; Daishe, W. Effects of organic matter removal on nitrogen and phosphorus ralease characteristic from surface sediments in urban shallow lakes. *Bulletin of Soil and Water Conservation* **2021**, *41*, 9-14+74, doi:10.13961/j.cnki.stbctb.2021.05.002.
29. Özacar, M. Adsorption of phosphate from aqueous solution onto alunite. *Chemosphere* **2003**, *51*, 321-327.
30. Wang, C.; Wang, Z.; Lin, L.; Tian, B.; Pei, Y. Effect of low molecular weight organic acids on phosphorus adsorption by ferric-alum water treatment residuals. *Journal of Hazardous Materials* **2012**, *203*, 145-150.